LAWRENCE
LIVERMORE
NATIONAL
LABORATORY

UCRL-JRNL-223562

Sub-nanometer-scale measurements of the interaction of ultrafast soft x-ray free-electron-laser pulses with matter

S. Hau-Riege, H. Chapman, J. Krzywinski, R. Sobierajski, R. London, R. Bionta, M. Bergh, C. Caleman, R. Nietubyc, L. Juha, J. Kuba, S. Bajt, E. Spiller, S. Baker, B. Kjornrattanawanich, E. Gullikson, T. Tschentscher, E. Plonjes, S. Toleikis

August 9, 2006

Physical Review Letters

Sub-nanometer-scale measurements of the interaction of ultrafast soft x-ray free-electron-laser pulses with matter

Stefan P. Hau-Riege[1], Henry N. Chapman[1], Jacek Krzywinski[2], Ryszard Sobierajski[2], Richard A. London[1], Richard Bionta[1], Magnus Bergh[3], Carl Caleman[3], Robert Nietubyc[2], Libor Juha[4], Jaroslav Kuba[5], Sasa Bajt[1], Eberhard Spiller[1], Sherry Baker[1], Benjawan Kjornrattanawanich[6], Eric Gullikson[7], Thomas Tschentscher[8], Elke Plönjes[8], and Sven Toleikis[8].

[1] Lawrence Livermore National Laboratory, Livermore, California 94550
[2] Institute of Physics PAS, Al. Lotników 32/46, PL-02-668 Warsaw, Poland
[3] Uppsala University, Uppsala, SE-75124 Sweden
[4] Institute of Physics AS CR, Na Slovance 2, 182 21 Prague 8, Czech Republic
[5] Czech Technical University, V Holešovičkách 2, 180 00 Prague 8, Czech Republic
[6] Brookhaven National Laboratory, Upton, New York 11973
[7] Lawrence Berkeley National Laboratory, Berkeley, California 94720
[8] Deutsches Elektronen-Synchrotron, DESY, Notkestraße 85, D-22607 Hamburg, Germany

Correspondence should be addressed to SPHR.

Femtosecond pulses from soft-x-ray free-electron lasers (FELs) [1] are ideal for directly probing matter at atomic length scales and timescales of atomic motion. An important component of understanding ultrafast phenomena of light-matter interactions is concerned with the onset of atomic motion which is impeded by the atoms' inertia. This delay of structural changes will enable atomic-resolution flash-imaging [2-3] to be performed at upcoming x-ray FELs [4-5] with pulses intense enough to record the x-ray scattering from single molecules [6]. We explored this ultrafast high-intensity regime with the FLASH soft-x-ray FEL [7-8] by measuring the reflectance of nanostructured multilayer mirrors using pulses with fluences far in excess of the mirrors' damage threshold. Even though the nanostructures were ultimately completely destroyed, we found that they maintained their integrity and reflectance characteristics during the 25-fs-long pulse, with no evidence for any structural changes during that time over lengths greater than 3 Å.

In the recently built FLASH FEL [7], x-rays are produced from short electron pulses oscillating in a periodic magnet array, called an undulator, by the principle of self-amplification of spontaneous emission [9-10]. The laser quality of the x-ray pulses can be quantified by the peak spectral brilliance of the source, which is 10^{28} photons/(s mm^2 mrad^2 0.1% bandwidth) [8]; this is up to seven orders of magnitude higher than modern third-generation synchrotron sources. For our studies, the machine operated with pulses of 25 fs duration at a wavelength of 32.5 nm and energies up to 21 μJ. We focused these pulses to $3\text{x}10^{14}$ W/cm^2 onto our nanostructured samples, resulting in an the unprecedented heating rate of $5\text{x}10^{18}$ K/s, while probing the irradiated structures at the nanometer length scale.

The x-ray reflectivity of periodic nanometer-scale multilayers [11] is very sensitive to changes in the atomic positions and the refractive indices of the constituent materials, making them an ideal choice to study structural changes induced by ultrashort FEL pulses. The large multilayer reflectivity results from the cooperative interaction of the x-ray field with many layers of precisely fabricated thicknesses, each less than the x-ray wavelength. This Bragg or resonant reflection from the periodic structure is easily disrupted by any imperfection of the layers. The characteristics of the structure, such as periodicity or layer intermixing, can be precisely determined from the measurement of the Bragg reflectivity as a function of incidence angle. These parameters can be easily measured to a small fraction of the probe wavelength, as is well known in x-ray crystallography where average atomic positions of minerals or proteins are found to less than 0.01Å. Thus, we

can explore ultrafast phenomena at length scales less than the wavelength, and investigate the conditions to overcome the effects of radiation damage by using ultrafast pulses.

For our measurements we fabricated multilayer mirrors consisting of ten alternating layers of silicon (257.8 Å thick) and carbon (17.5 Å), by sputter deposition onto a silicon wafer. A transmission electron micrograph of a cross section of the multilayer is shown in Fig. 1 (b). In this image the thin carbon layers show up bright in between the thicker silicon layers. We purposely designed the multilayer to minimize the amount of x-ray absorbing carbon, to provide the maximum penetration of the 32.5 nm light through the structure. In this way the FEL pulse interacts with the most periods, which results in the narrowest Bragg reflection peak and provides us with the highest sensitivity to structural changes achievable with these materials and wavelength. We achieved a further narrowing of the peak by performing the measurement with the plane of reflection parallel to the electric-field vector of the linearly polarized FEL pulse (*p*-polarization) [12].

Our experimental arrangement is illustrated in Fig. 1 (a) [13]. The beam was focused onto our multilayer sample to a spot with a full-width-at-half-maximum of approximately 17±2 μm for an angle of incidence of the sample of 45^{o} at the mirror surface. This diameter was determined by measuring the area of the damaged region as a function of incoming pulse energy [14].

Incident pulses with fluences greater than about 0.3 J/cm^2 destroy the multilayer structure and leave craters in the substrate. A Nomarski differential-interference-contrast micrograph of an exposed spot is shown in Fig. 1 (e). This optical microscope is sensitive to phase differences across the sample, which in this case allows us to visualize the gradient of the crater depth . The terraces that are observed are individual layer groups that are ablated, as can also be seen in cross-sectional TEM micrographs in Fig. 1 (c). Near the threshold of damage layers ablate (A), recrystallize (B), and interdiffuse (C), possibly accompanied by melting.

We measured the energy of the reflected pulse, for various off-normal angles of incidence θ ranging from 38° to 52°, as a function of pulse energy. Each single-pulse measurement was performed on a clean, unexposed area of the mirror. The angular dependence of the reflectivity is shown in Fig. 2 (a) for incident pulses attenuated to less than 0.1 J/cm^2. At this fluence we did not observe damage in the multilayer, and the reflectivity is in agreement with that measured synchrotrons calculation [15]. The reflectivity for a larger range of fluences is shown in Fig. 2 (b), grouped according to the incident pulse fluence. We found that for all measured fluences up to 6.6 J/cm^2, the angular position of the peak reflectivity does not change by more than the measurement tolerance of 1° corresponding to a change in period no more than 3 Å. Fig. 2 (c) shows the reflectivity within the range $44° \leq \theta \leq 47°$ plotted as a function of fluence. The reflectivity of the multilayer decreases somewhat with increasing fluence.

We gained a deeper understanding of the multilayer damage mechanism through computations. We calculated the standing-wave intensity distribution inside the multilayer structure using steady-state methods based on Fresnel equations [16]; these time-independent models are applicable since the time for the light to propagate a few attenuation lengths (approximately 2 fs) is much shorter than the pulse length (25 fs). We based our estimate of the complex index of refraction of the multilayer materials on published room-temperature solid-density values [17], and corrected for the dependence on the temperature and density using an average ion model employing screened hydrogen potentials [18-19]. Finally, we calculated the hydrodynamic explosion of the multilayer using the HYDRA radiation hydrodynamics code [20]. This model accounts for radiation transport and electron thermal conduction.

Our calculations show that the 32.5 nm radiation light first heats the electrons in the multilayer, as shown in Fig. 3 (a). In our minimum absorption multilayer design, at the angle of incidence for peak reflectivity the nodes of the light intensity reside in strongly absorbing carbon-containing layers, whereas the high-intensity antinodes reside in the more transparent silicon. Therefore the radiation field and the electron heating are much larger in the thick silicon layers than in the layers containing carbon. Since the electrons are not able to transfer a

significant amount of energy to the ions before the pulse ends, the ions do not move initially. The calculated motion of the material in the multilayer is shown in Fig. 3 (b). The multilayer explodes on a timescale of picoseconds but stays intact during the pulse: the thermal velocity of a silicon atom at the end of the pulse is $v \sim \sqrt{3kT_{ion}/m_{ion}} \sim 0.023$Å / fs for $kT_{\mathrm{ion}} = 0.5$ eV; during the 25fs pulse, the ions can move only about 0.3Å. Since this is much less than the smallest layer thickness it is not expected that the multilayer will be significantly distorted, the layers interdiffuse, nor that substantial changes in the atomic positions will occur that lead to changes in the crystallographic form factor. Therefore, the drop in reflectivity for large fluences as shown in Fig. 2 (c) is not likely to be caused by atomic motion. This reflectivity drop is primarily a consequence of a change in the index of refraction of the multilayer materials induced by heating of the electrons and/or ionization.

The possibility of overcoming the damage barrier by applying short pulses has significant technological interest. For x-rays, multilayer coatings can provide optics of higher numerical aperture (resulting in smaller focal spots) than uncoated mirrors. Extremely high focusing will be required for the application of XFELs to bio-molecular imaging or the creation and observation of extreme conditions in matter, such as exotic excited states of atoms and warm dense plasmas [21]. To date, the smallest x-ray focal spots of 30 nm diameter at 19.5keV photon energy have been achieved with thick multilayer structures, operating in a Laue (transmission) geometry [22]. It is predicted that these multilayer Laue lenses will produce spot sizes below 5 nm, and hence could be used to focus XFEL pulses to achieve x-ray power densities of 3×10^{22} W/cm^2, assuming anticipated XFEL light output [5]. This corresponds to electric-field strengths close to the Schwinger critical field, at which spontaneous electron-positron pair creation is expected to take place, amounting to "boiling the vacuum" [23]. These lenses are only several hundred micrometer in diameter, and so will necessarily be exposed to high incident power densities, where damage will occur, but not before carrying out their function.

Our experiments on the interaction of intense FEL pulses with precise nanometer-scaled resonantly reflecting structures show that these structures maintain their integrity during the pulse. In this sense, our findings demonstrate that the multilayer functions nearly without any degradation under high-power FEL irradiation, since the pulse length is short enough that structural damage does not occur over the duration of the pulse. This experiment is the first demonstration that it is possible for structural damage to occur on a timescale that is larger than the duration of intense FEL pulses. Important applications of this concept are single molecule diffraction, where uncrystallized macromolecules could be imaged at doses five orders of magnitude above the conventional damage threshold [6], and in greatly extending the capabilities of FELs through the use of single-pulse optics.

Acknowledgements

We thank the FLASH staff at DESY for facilitating these experiments, Richard Lee, Klaus Sokolowski-Tinten, and Nikolai Stojanovic for helpful discussions, and Jennifer Alameda for assistance in the fabrication of the multilayer mirrors. This work was performed under the auspices of the US Department of Energy by the University of California, Lawrence Livermore National Laboratory under Contract No. W-7405-Eng-48. This work was partially funded also by the Czech Ministry of Education within the framework of programs INGO (Grant 1P2004LA235) and National Research Centers (Projects LC510 and LC528).

References

[1] Madey, J.M.J., "Stimulated emission of bremsstrahlung in a periodic magnetic field", *J. Appl. Phys.* **42**, 1906-1913 (1971).
[2] Solem, J.C. and Chapline, G.F., "X-ray biomicroholography", *Opt. Eng.* **23**, 193-203 (1984).
[3] Solem, J.C. and Baldwin, G.C., "Microholography of living organisms", *Science* **218**, 229-235 (1982).
[4] Richard, F., Schneider, J.R., Trines, D., and Wagner, A., "TESLA Technical Design Report", March 2001, available at the web site http://tesla.desy.de/new_pages/TDR_CD/start.html.
[5] Linac Coherent Light Source (LCLS) Design Study Report, SLAC-R-521, 1998, available from the National Technical Information Services, 5285 Port Royal Road, Springfield, Virginia, 22161, also available online at: http://www-ssrl.slac.stanford.edu/lcls/design_report/e-toc.html.
[6] Neutze, R., Wouts, W., van der Spoel, D., Weckert, E., and Hajdu, J., "Potential for biomolecular imaging with femtosecond x-ray pulses", *Nature* **406**, 752-757 (2000).
[7] Formerly known as VUV-FEL.
[8] Ayvazyan, V. *et al*., "First Operation of a free-electron laser generating GW power radiation at 32 nm wavelength", *Eur. Phys. J. D* **37**, 297-303 (2006).
[9] A. Kondratenko and E. Saldin, *Part. Accel*. **10**, 207 (1980).
[10] Feldhaus, J. et al., "The Infrared Undulator Project at the VUV-FEL", *Proceedings of the 27th International Free Electron Laser Conference* (FEL 2005), Stanford, U.S.A., Aug 2005, p. 183 - 186.
[11] Spiller, E., "Low-loss reflection coatings using absorbing materials", *Appl. Phys. Lett.* **20**, 365-367 (1972).
[12] A. Authier, "Dynamical Theory of X-Ray Diffraction", IUCr Crystallographic Symposia, Oxford University Press, New York (2001).
[13] Tiedtke, K. et al., "The SASE FEL at DESY: Photon Beam Diagnostics for the User Facility, *Proceedings SRI2003*, San Francisco, AIP Conf. Proc. 705, 588-592 (2004).
[14] Liu, J.M., "Simple technique for measurements of pulsed Gaussian-beam spot sizes", *Opt. Lett.* **7**, 196-198 (1982).
[15] Advanced Light Source (ALS), High-Precision EUV Calibration and Standards Beamline 6.3.2. Similar results were obtained at the National Synchrotron Light Source (NSLS), Beamline X24C.
[16] Windt, D.L., "IMD – Software for modeling the optical properties of multilayer films", *Comp. Phys.* **12**, 360-370 (1998).
[17] Henke, B.L., Gullikson, E.M., and Davis, J.C, "X-ray interactions: photoabsorption, scattering, transmission, and reflection at E=50-30000 eV, Z=1-92", *Atom. Nucl. Data Tabl*. **54**, 181-342 (1993).
[18] Zimmerman, G. B. and More, R. M., "Pressure ionization in laser-fusion target simulation", *J. Quant. Spectrosc. Radiat. Transf*. **23**, 517-522 (1980).
[19] More, R. M., "Electronic energy-levels in dense plasmas", *J. Quant. Spectrosc. Radiat. Transf*. **27**, 345-357 (1982).
[20] Marinak, M.M. *et al*., "Three-Dimensional HYDRA simulations of National Ignition Facility Targets", *Phys. Plasmas*. **8**, 2275-2280 (2001).
[21] Shenoy, G.K. and Stöhr, J., eds., "LCLS – The First Experiments", SSRL (2000), available at the web site http://www-ssrl.slac.stanford.edu/lcls/papers/lcls_experiments_2.pdf
[22] Kang, H. C. *et al*., "Nanometer Focusing of Hard X-rays by a Multilayer Laue Lens," *Phys. Rev. Lett.* **96**, 127401 (2006).
[23] M. Marklund and P.K. Shykla, "Nonlinear collective effects in photon-photon and photon-plasma interactions", *Rev. Mod. Phys*. **78**, 591-640 (2006).

Figure Legends:

Figure 1: (a) Experimental geometry (top-down view), showing the beam path from FEL undulator through a gas cell (to selectively attenuate the pulse energy by up to a factor of 100) and transparent gas ionization detector (to measure incident pulse energy) before focusing onto the sample with an ellipsoidal mirror [13]. The energy of the pulse reflected from the sample is detected with a photodiode with 1.5° angular acceptance. (b) A TEM image of a cross-section of the multilayer nanostructure in an undamaged region, in which the 10 layers of 27.5 nm period can be seen. (c) and (d) TEM image of cross sections of the nanostructure at different positions within the FEL-exposed spot. The positions are as indicated in (e), which is a Nomarski differential-interference-contrast micrograph of the multilayer surface. In (d), the multilayer structure and 400 nm of the substrate were ablated.

Figure 2: (a) Low-fluence reflectivity as a function of the off-normal angle of incidence θ measured at FLASH. Overlaid is the data measured at the synchrotron [ALS] at a very low flux of less than 1.5 $\mu W/cm^2$ and the calculated reflectivity (solid line). For both we assumed that the incident light consisted of 90% p-polarized light and 10% s-polarized light. (b) Reflectivity as a function of the off-normal angle of incidence θ at higher fluences. In this second set of experiments, we observed an angular shift of 1 degree with respect to the measurements shown in (a). This could be due to a difference in wavelength of about 0.6 nm, which is consistent with the FEL operation. (c) Multilayer reflectivity ranging from 44 to 47 degrees (data taken from (b)) as a function of pulse energy. A linear fit through the data is shown as a thick solid line, and the 90% confidence level for this fit as thin lines. This fit suggests that the reflectivity drop at the high-fluence end lies between 7 and 41%. Overlaid as a dashed line are the simulation results.

Figure 3: Computational results assuming a pulse energy of 20 μJ, a pulse length of 25 fs, and a beam diameter of 17 μm. (a) Spatial dependence of electron and ion temperatures at different times during the pulse. (b) Position of the bilayer interfaces of the multilayer as a function of time during irradiation (left) and afterward (right).

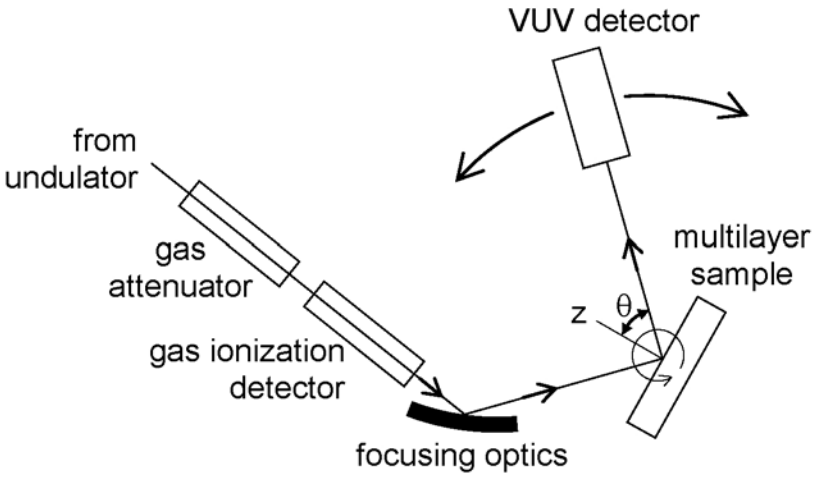

Figure 1 (a)

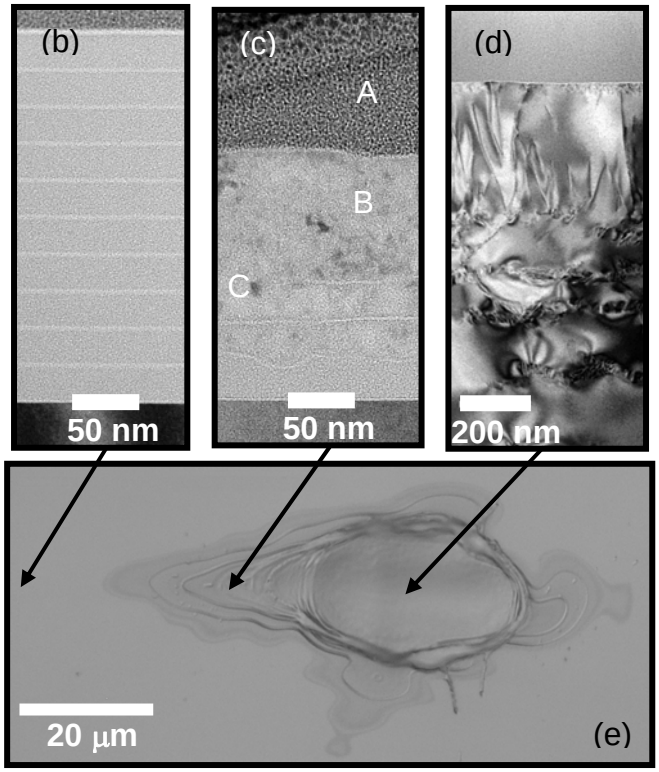

Figure 1 (b) to (e)

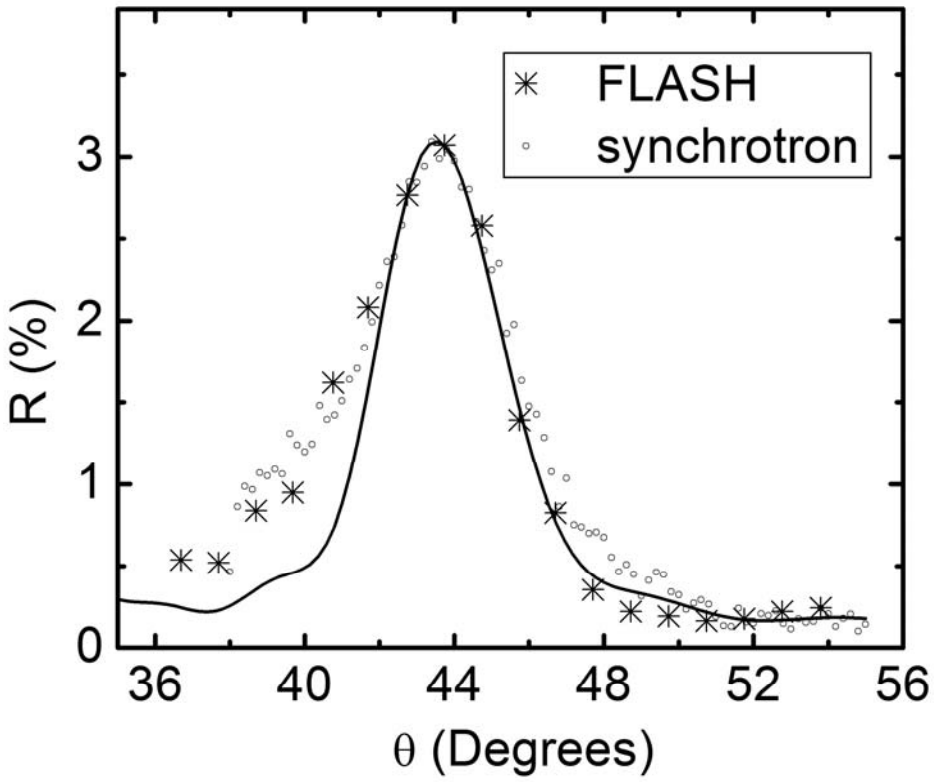

Figure 2 (a)

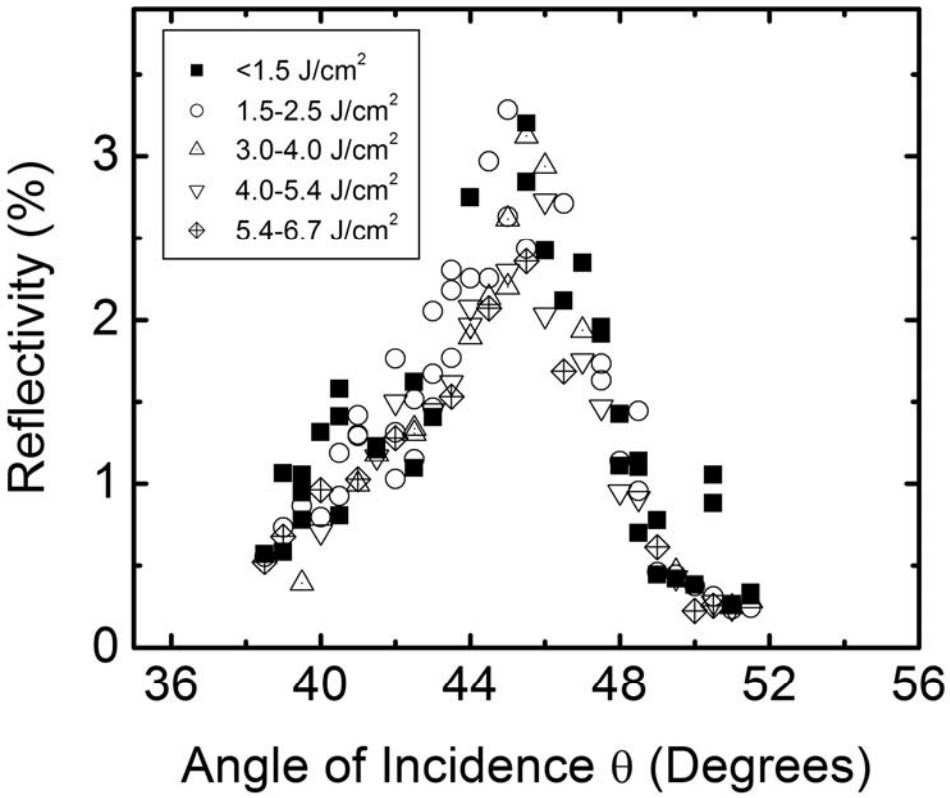

Figure 2 (b)

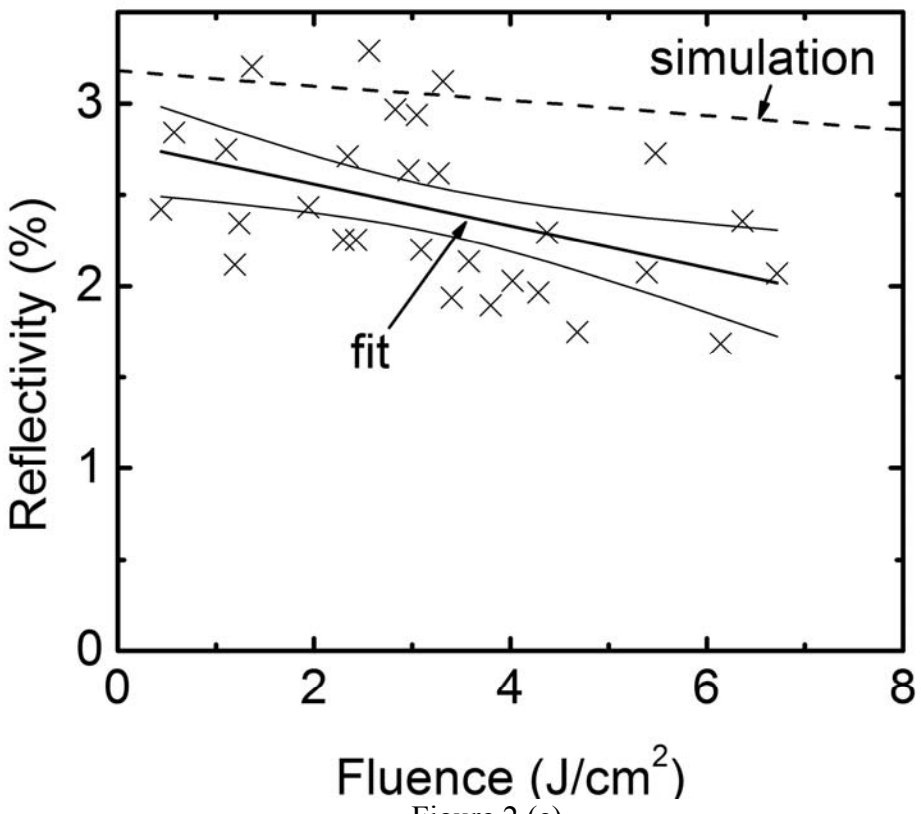

Figure 2 (c)

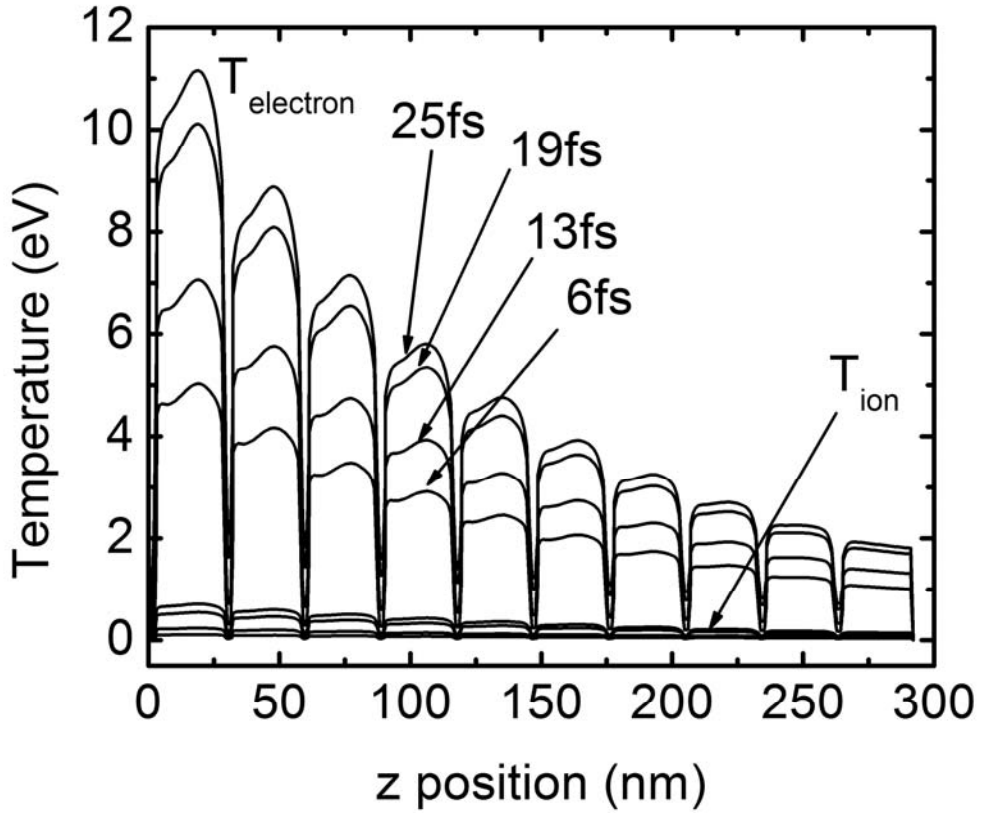

Figure 3 (a)

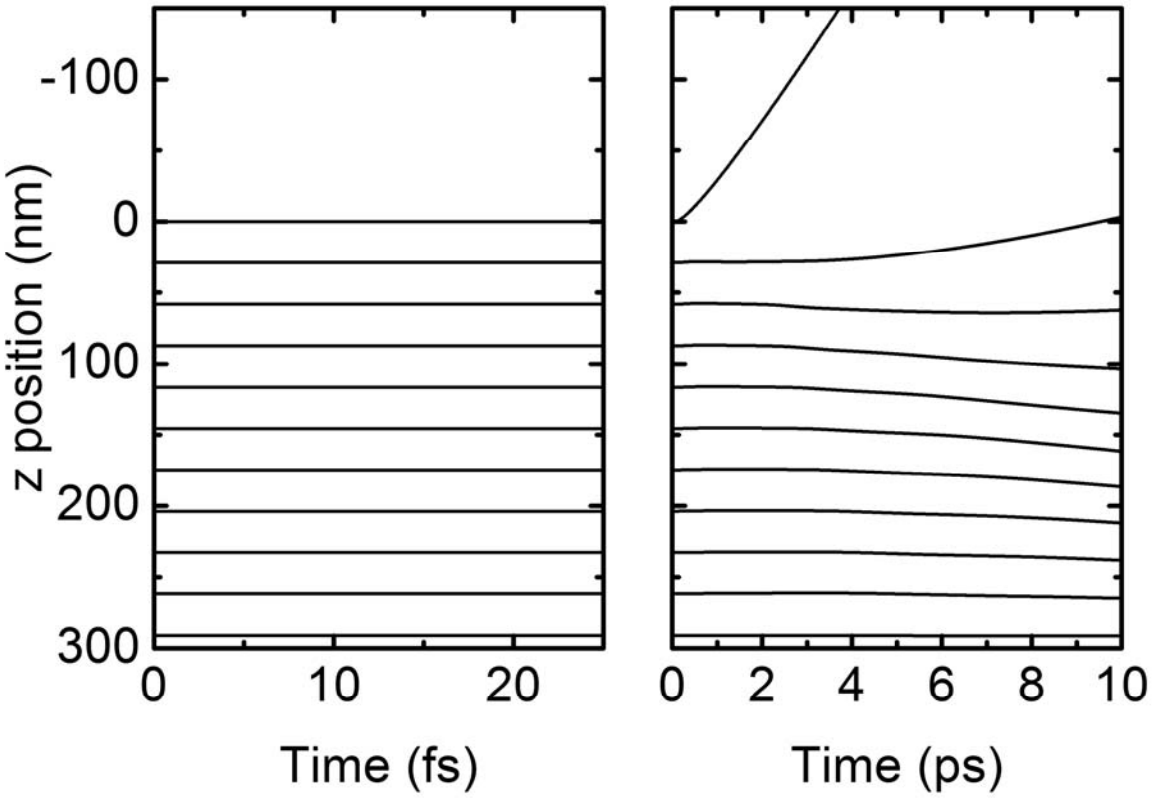

Figure 3 (b)